Vrije Universiteit Brussel

Effect of core-shell structuring of chabazite zeolite with a siliceous zeolite thin layer on the separation of acetone-butanol-ethanol vapor in humid vapor conditions

Miyamoto, Manabu; Iwatsuka, Haruna; Oumi, Yasunori; Uemiya, Shigeyuki; Van der Perre, Stijn; Baron, Gino V.; Denayer, Joeri F. M.

Published in:
Chemical Engineering Journal

DOI:
10.1016/j.cej.2019.01.106

Publication date:
2019

License:
CC BY-NC-ND

Document Version:
Accepted author manuscript

Link to publication

Citation for published version (APA):
Miyamoto, M., Iwatsuka, H., Oumi, Y., Uemiya, S., Van der Perre, S., Baron, G. V., & Denayer, J. F. M. (2019). Effect of core-shell structuring of chabazite zeolite with a siliceous zeolite thin layer on the separation of acetone-butanol-ethanol vapor in humid vapor conditions. *Chemical Engineering Journal*, *363*, 292-299. https://doi.org/10.1016/j.cej.2019.01.106

Copyright
No part of this publication may be reproduced or transmitted in any form, without the prior written permission of the author(s) or other rights holders to whom publication rights have been transferred, unless permitted by a license attached to the publication (a Creative Commons license or other), or unless exceptions to copyright law apply.

Take down policy
If you believe that this document infringes your copyright or other rights, please contact openaccess@vub.be, with details of the nature of the infringement. We will investigate the claim and if justified, we will take the appropriate steps.

Download date: 19. Apr. 2024

Chemical Engineering Journal 363 (2019) 292–299

Contents lists available at ScienceDirect

Chemical Engineering Journal

journal homepage: www.elsevier.com/locate/cej

Effect of core-shell structuring of chabazite zeolite with a siliceous zeolite thin layer on the separation of acetone-butanol-ethanol vapor in humid vapor conditions

Manabu Miyamoto[a,*], Haruna Iwatsuka[b], Yasunori Oumi[c], Shigeyuki Uemiya[a], Stijn Van den Perre[d], Gino V. Baron[d], Joeri F.M. Denayer[d,*]

[a] Department of Chemistry and Biomolecular Science, Gifu University, 1-1 Yanagido, Gifu 501-1193, Japan
[b] Department of Materials Science and Technology, Gifu University, 1-1 Yanagido, Gifu 501-1193, Japan
[c] Research Equipment Sharing Promotion Center, Gifu University, 1-1 Yanagido, Gifu 501-1193, Japan
[d] Department of Chemical Engineering, Vrije Universiteit Brussel, Pleinlaan 2, Brussels 1050, Belgium

HIGHLIGHTS

- A chabazite aluminosilicates coated with a siliceous chabazite layer was synthesized.
- Adsorption rate of 1-butanol was decreased by the pure silica chabazite coating.
- Coated chabazite showed an even more pronounced exclusion of 1-butanol.
- Pure silica chabazite coating layer acts as a diffusion barrier.

ARTICLE INFO

Keywords:
Biobutanol
Adsorption
Chabazite zeolite
Core-shell
ABE
Molecular sieving

ABSTRACT

Due to its shape selective properties, the narrow pore chabazite zeolite is an interesting material for the separation and purification of 1-butanol from ABE (acetone-butanol-ethanol) fermentation broth, as it selectively traps ethanol from the mixture of acetone, ethanol and butanol. In order to improve the separation performance of chabazite zeolite in humid conditions, we synthesized a core-shell structured chabazite type zeolite, with a chabazite aluminosilicate core coated with a pure silica chabazite layer. This material was evaluated in the vapor phase separation of 1-butanol using a model ABE vapor mixture. Unexpectedly, a broader breakthrough profile of ethanol was obtained on the coated chabazite, resulting in a lower 1-butanol recovery. It was found that the adsorption rate of 1-butanol was decreased by the pure silica chabazite coating. In breakthrough experiments, the coated chabazite showed an even more pronounced exclusion of 1-butanol as compared to the parent material, resulting in a larger separation factor of ethanol over 1-butanol. The pure silica chabazite coating layer acts as a kind of diffusion barrier against 1-butanol rather than ethanol, enhancing the molecular sieving effect.

1. Introduction

Biobutanol (or 1-butanol produced by fermentation of biomass) is considered as an interesting platform molecule and a potential energy source because of its superior properties as compared to ethanol. The fermentative production of 1-butanol from renewable feedstocks, which is called the ABE (acetone-butanol-ethanol) fermentation, has received considerable attention as a sustainable alternative to fossil sources and typically produces a mixture of acetone, 1-butanol and ethanol. Unfortunately, production of biobutanol by fermentation is hampered by serious end-product inhibition with only 2–3 wt% of butanol in water [1]. Because of the low content of butanol, there still is a challenge to develop cost-effective separation techniques. Conventional distillation processes for the biobutanol recovery from ABE fermentation broth require more energy than the energy content recovered from biobutanol [1–4]. Adsorptive separation of the ABE mixture was identified as the most energy-efficient technique [5]. Thus, many researchers investigated the adsorptive separation of butanol from fermentation media or from aqueous model solutions using a wide range of adsorbent materials including activated carbon [6–8], polymeric

* Corresponding authors.
E-mail addresses: m_miya@gifu-u.ac.jp (M. Miyamoto), joeri.denayer@vub.ac.be (J.F.M. Denayer).

https://doi.org/10.1016/j.cej.2019.01.106
Received 26 November 2018; Received in revised form 17 January 2019; Accepted 21 January 2019
Available online 22 January 2019
1385-8947/ © 2019 Elsevier B.V. All rights reserved.

resins [5–7], zeolites [5,7,8–11] and metal-organic frameworks (MOFs) [10–13].

Among those materials, chabazite (CHA) type zeolites offer interesting properties for the separation and purification of 1-butanol. CHA type zeolites are composed of double 6MR units connected to ellipsoidal large cage (6.7 × 10 Å), resulting in a three-dimensional pore system with an 8MR window of 3.8 × 3.8 Å. Because of this small pore system, CHA type zeolites show distinctive shape selective properties. In previous work, we demonstrated a clear cut-off in adsorption capacity of 1-alcohols between C2 and C3 on CHA type aluminosilicate and SAPO-34 (silicoaluminophosphate with CHA topology) in liquid phase adsorption [14,15]. Cousin Saint Remi et al. experimentally investigated the intracrystalline diffusivity of 1-alcohols in SAPO-34 zeolite in liquid phase [17]. A significant difference in the intracrystalline diffusion coefficients between ethanol (1.6×10^{-14} m^2/s) and 1-propanol (3.5×10^{-18} m^2/s) was observed. It was concluded that the small dimensions of the SAPO-34 framework generate a very sterically hindered diffusion of 1-alcohols into the crystals, resulting in a chain-length-dependent behavior, interesting to obtain efficient kinetic-based separations. Krishna and van Baten, using configurational-bias Monte Carlo (CBMC) simulations, also found this chain length dependent adsorption and diffusion mechanism [16].

Those studies mentioned above considered adsorption processes under liquid conditions. Recently, vapor phase adsorptive separation of 1-butanol gained interest, because the combination of gas stripping and adsorption has some specific advantages [18–20]. In comparison to liquid phase adsorption, operation in the vapor phase results in a higher ABE concentration relative to water, fewer competitive effects as the composition of the vapor is much less complex than that of the fermentation broth and less stability issues for adsorbents. Recently, Van der Perre et al. reported a two-step adsorptive separation using pure silica LTA and SAPO-34, achieving high butanol recovery and purity from the vapor head phase of ABE fermentation broth [21]. In this study, pure silica CHA also offered high ethanol selectivity over 1-butanol, because the pore size of CHA leads to exclusion or very slow diffusion of 1-butanol.

In previous work, some of us have developed core-shell structured MFI type zeolites, consisting of a catalytically active ZSM-5 core coated with a thin layer of silicalite-1 (pure silica MFI type zeolite), exhibiting unprecedented product selectivity in chemical reactions [22–24]. Recently, core-shell structured MFI type zeolite demonstrated remarkably high water tolerance and stable CO_2 adsorption capacity even in the presence of saturated water vapor without an additional thermal treatment [25]. The presence of an all silica MFI layer at the surface of the material is expected to render the material more hydrophobic, resulting in a lower affinity for polar molecules such as water.

Various other authors have developed core-shell type zeolites to enhance or modify the material properties [26–31]. These studies indicate that core-shell structuring (coating of a pure silica zeolite thin layer) strongly affects the adsorption performance and molecular sieving effect of zeolites.

In this study, we developed a core-shell structured chabazite zeolite, with a core consisting of chabazite with a Si/Al ratio of 39, coated with pure silica chabazite zeolite. The synthesis of a hybrid material with a hydrophilic core and a hydrophobic shell layer was aimed at, as it was expected to show high water vapor tolerance with comparable adsorption capacity on the hydrophilic core material in ABE separation in humid conditions.

2. Experimental

2.1. Materials

Ludox® AS-40 colloidal silica was purchased from Aldrich. Aluminum hydroxide and hydrofluoric acid (HF) were purchased from Wako Pure Chemical Industries, Ltd. *N,N,N*-trimethyl-1-adamantylammonium hydroxide (TMAdaOH) solution was purchased from SACHEM, Inc. All reagents were used without further treatments.

2.2. Preparation of chabazite aluminosilicate

Chabazite aluminosilicate was synthesized by a modified method of pure silica chabazite synthesis according to the literature [32]. A precursor synthesis sol was prepared with the composition of 1 SiO_2: 0.017 Al_2O_3: 1.4 HF: 1.4: TMAdaOH. The prepared sol was dried at 373 K to remove excess water and the content of water (H_2O/SiO_2) in the dried powder was determined by thermogravimetry–differential thermal analysis (TG–DTA). Then, deionized water was added to the dried powder in order to adjust the final sol composition with 1 SiO_2: 0.017 Al_2O_3: 1.4 HF: 1.4: TMAdaOH: 4.5 H_2O and mixed vigorously at room temperature. Then, the mixture was introduced into a Teflon®-lined stainless-steel vessel for hydrothermal reaction at 448 K for 24 h. The product was filtered, washed by deionized water, dried at 373 K and calcined 853 K for 12 h.

2.3. Core-shell structuring of chabazite

A siliceous chabazite zeolite coating was performed by a secondary growth using a similar procedure as for CHA aluminosilicate synthesis. The synthesis sol was prepared by the same procedure as for CHA aluminosilicate synthesis with the molar composition of 1 SiO_2: 1.4 HF: 1.4: TMAdaOH: 7.5 H_2O and chabazite aluminosilicate crystals were mixed in the synthesis sol with the weight ratio of chabazite to SiO_2 in the sol equal to 1.84. The product was filtered, washed by deionized water, dried at 373 K and calcined 853 K for 12 h. The parent chabazite aluminosilicate and core-shell structured one are denoted as “parent CHA” and “coated CHA”, hereafter.

2.4. Characterization

The products were identified by their X-ray diffraction (XRD) pattern recorded on a Bruker D8 (Bruker AXS K.K.) using Cu Kα radiation. Crystal size, morphology and Si/Al ratio of the samples was assessed by scanning electron microscopy (SEM, Hitachi S-4800; Hitachi High-Technologies Corporation) equipped with an energy dispersive X-ray spectrometry (EDX, EMAX; HORIBA, Ltd.). Ar adsorption/desorption isotherms were measured using a Quantasorb Autosorb I device (Quantachrome Instruments) at 87 K. Before the measurements, all samples were degassed at 623 K under vacuum. The micropore volume was determined by the Gurvich rule.

p-Xylene cracking was performed using a fixed bed reactor with 30 mg of samples at 673 K to evaluate the catalytic activity of the external crystal surface. The samples were activated at 673 K for 1 h before starting the reaction. Then, p-xylene vapor was supplied by Ar bubbling into the reactor. The partial pressure of p-xylene and W/F were 1 kPa and 5000 g-cat min/mol, respectively. The products were analyzed by online gas chromatograph equipped with a FID detector (GC-14B, Shimadzu Corporation) using a ZB-WAXplus capillary column (Phenomenex).

2.4.1. Vapor phase adsorption measurements

Vapor phase adsorption isotherms of water and organic compounds (ethanol and 1-butanol) were measured at 313 K by a dynamic gravimetric method on an SGA-100H microbalance system (VTI corporation, USA). Samples were activated at 623 K for 6 h under a nitrogen flow. Vapor of water or organic compounds was supplied by N_2 bubbling through the temperature-controlled reservoir. Details can be found elsewhere [33].

2.4.2. Breakthrough curve measurements

Breakthrough curves were measured using packed columns with a mixture of quartz beads and the zeolite samples. The experimental

method is described elsewhere [34]. Ethanol/water, 1-butanol/water and acetone/ethanol/butanol/water mixtures were generated by flowing He through two metal reservoirs containing water and organic (ethanol, butanol or ABE mixture), respectively. Separately generated organic and water vapor were joined together and introduced continuously into the column. The concentration of the organic compounds in the effluent of the column was determined using an online gas chromatograph equipped with a FID detector and an automatic injection valve. The breakthrough profile of water vapor was also measured on the same set-up but using a TCD detector. The breakthrough experiments were performed at temperatures from 313 K to 373 K. Separation factor α_{ij} is calculated as following;

$$\alpha_{ij} = \frac{q_i/q_j}{p_i/p_j}$$

where q_i is an amount adsorbed of component i and p_i is a vapor pressure of component i.

3. Results and discussion

3.1. Characterization of parent and coated CHA

The products before and after the pure silica chabazite coating were identified as CHA type zeolite and no other crystal phase was identified from the XRD patterns as shown in Fig. 1. Both parent and coated CHA were pseudo cubic in shape as shown in Fig. 2. The crystal size was slightly larger after coating and the Si/Al ratio of the crystals also increased from 39.3 to 40.6. These results indicate a pure silica chabazite layer could be formed by the secondary growth on the crystals of the parent CHA, and its layer thickness was estimated to be approximately 100 nm from the difference in average crystal sizes in Table 1. The theoretical Si/Al ratio of the hybrid core-shell material is 45.9 on the assumption of 100 nm thickness of the pure silica CHA shell layer. This theoretical value is slightly different from the EDX results as shown in Table 1. This would be due to relatively low energy resolution of EDX and low Al content. In the case of the coated CHA, small pseudo cubic crystals were also observed, as can be seen in Fig. 2b. The Al content of these small crystals was under detection limits. Thus, these crystals were probably pure silica chabazite, nucleated separately from chabazite core crystals in the synthesis sol. From Ar adsorption/desorption measurements, the micropore volumes of parent and coated CHA were 0.21 and 0.25 cm^3/g, respectively. The slightly higher micropore volume of coated CHA would be owing to the relatively high crystallinity (13% higher than the parent CHA) or presence of amorphous like materials for the parent CHA as can be seen in Fig. 2a (indicated by circles).Fig. 3.

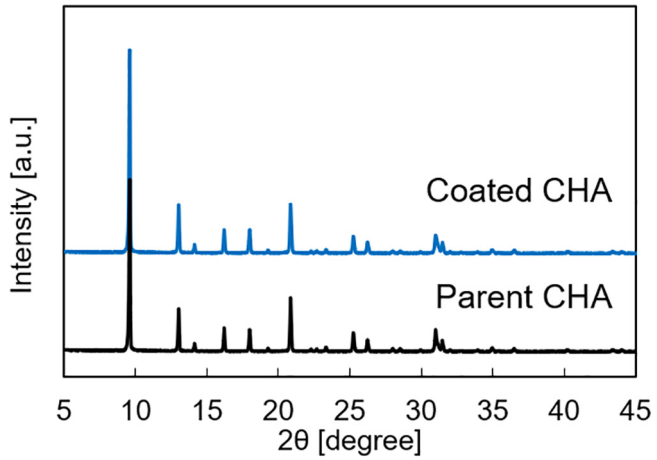

Fig. 1. XRD patterns of parent and coated CHA.

Cracking of *p*-xylene was performed to evaluate catalytic activity on an external surface of crystals, because *p*-xylene is too large to diffuse in the pores of CHA. The conversion of *p*-xylene was 41.0% on the parent CHA, indicating catalytically active sites derived from Al in the framework were present on the external surface of the crystals. In contrast, the *p*-xylene conversion was significantly decreased to 0.2% by the pure silica CHA coating. This clearly shows the catalytically inactive siliceous CHA thin layer could successfully cover the parent CHA and deactivate the active sites on the external surface of the parent CHA crystals.

3.2. Vapor phase adsorption isotherms

The vapor phase adsorption isotherms of ethanol, butanol and water are shown in Fig. 4. Both materials exhibited type I isotherms for ethanol adsorption. The maximum adsorption capacity on the parent CHA was 3.1 mmol/g, which is consistent with the value of 2.9 mmol/g on pure silica chabazite reported by Van der Perre et al. [21] The adsorbed amount of ethanol on the parent CHA and the coated CHA is comparable at low relative pressures, but at higher relative pressure, the coated CHA material exhibited higher adsorption capacity. The higher adsorbed amount on the coated CHA in high partial pressures could be explained by its higher micropore volume. However, a larger capacity would also be expected at low pressure, which is not the case. Also for 1-butanol, the capacity of the coated sample exceeds that of the parent material at intermediate to high pressure, but not at low pressure. It should be noted that the adsorbed amount of butanol was not in equilibrium, even after 1500 min of the equilibrium time because of its extremely slow uptake kinetics [21]. Thus, the difference in adsorbed amount in the *pseudo*-isotherms is greatly affected by the adsorption kinetics of 1-butanol. At low partial pressures, for instance, the uptake kinetics of butanol were faster on the parent CHA than that on the coated one, as shown in Fig. 4d. Thus, the discrepancy in behavior between low and high pressure can be explained by very slow diffusion with the coated sample, which makes it difficult to reach full equilibrium at low pressure.

In the case of water vapor adsorption, less difference in uptake between the parent and coated CHA was observed. The slightly lower adsorbed amounts on the coated CHA could be explained by the hydrophobic pure silica CHA coating, but this effect is very limited.

3.3. Vapor phase breakthrough curves of single alcohols in humid conditions

Breakthrough profiles of pure ethanol and 1-butanol vapor diluted in He and in humid conditions (water vapor pressure of 4.2 kPa) are shown in Fig. 5. While a sharp breakthrough profile of ethanol is obtained on the parent CHA, significant broadening is observed with the coated sample. The adsorbed amounts of ethanol at 313 K were 1.52 and 1.46 mmol/g on the parent and coated CHA, respectively. Those values are comparable to the values of the adsorption isotherms. Additionally, estimated occupancy by water adsorbed at 4.2 kPa from the adsorption isotherm was only 35.5 and 29.0% in total pore volume for the uncoated and coated CHA, respectively, whereas those by the ethanol amount adsorbed were 41.2 and 33.5%. Thus, in the present conditions, the presence of water vapor did not inhibit the adsorption of ethanol on both samples. Thus no beneficial effect of the hydrophobic pure silica CHA coating layer with respect to water sensitivity occurs. In fact, DFT calculations evidenced the interaction energy of ethanol at very low degree of pore filling in pure silica CHA is much higher than that of water [21].

For 1-butanol, breakthrough occurs very rapidly because this molecule is sterically hindered in the narrow pores of chabazite and diffuses very slowly. This effect is even more pronounced on the coated sample, where butanol breakthrough occurs even faster. These results indicate that all-Si CHA coating introduces a mass transfer resistance.

For ethanol, breakthrough experiments were also performed at

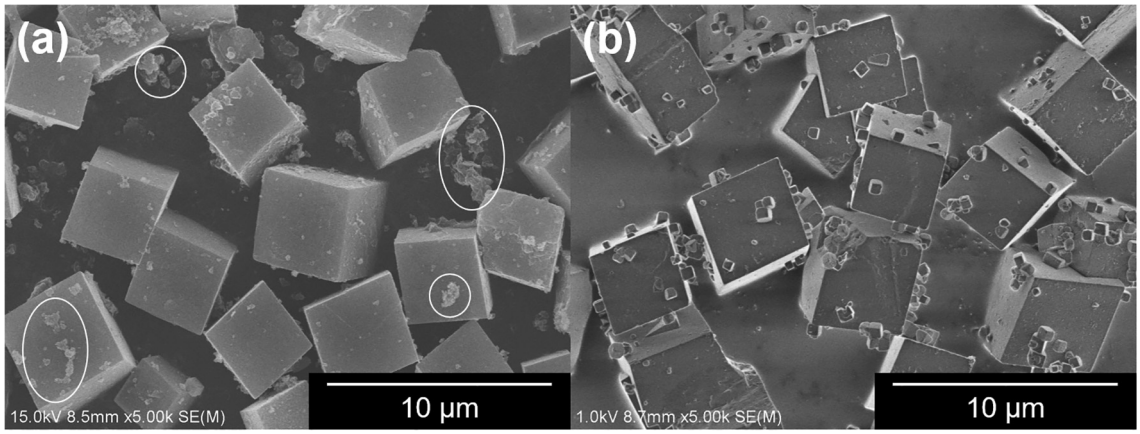

Fig. 2. SEM images of parent (a) and coated CHA (b). Circles indicates amorphous like materials.

different temperatures (Fig. 6a-d). As expected, the breakthrough time decreases with increasing temperature, because of the decrease in capacity with temperature. For the parent CHA, the shape of the breakthrough profiles is not affected by temperature, indicating ethanol adsorption occurs in absence of diffusion limitations (see Fig. 6a and c). In contrast, the normalized breakthrough profiles of ethanol became slightly broader on the coated CHA (Fig. 6b and d). The lower driving force for adsorption at higher temperature together with the presence of a diffusion resistance results in breakthrough curve broadening. The pure silica CHA shell layer most probably reduces the uptake rate of molecules as it suppresses the strong surface adsorption sites which are present on the external surface of CHA core crystals, owing to Al species and compensation cations. This would result in lower driving force for adsorption of alcohols into zeolites. Another possibility is the marginally smaller pore openings of zeolites with increasing framework Si/Al ratio, because the higher content of metal species in the framework enlarges the lattice spacing of zeolites. In fact, the d(1000)-spacing is 0.3% declined between ZSM-5 with Si/Al of 35 and purely siliceous silicalite-1 [35].

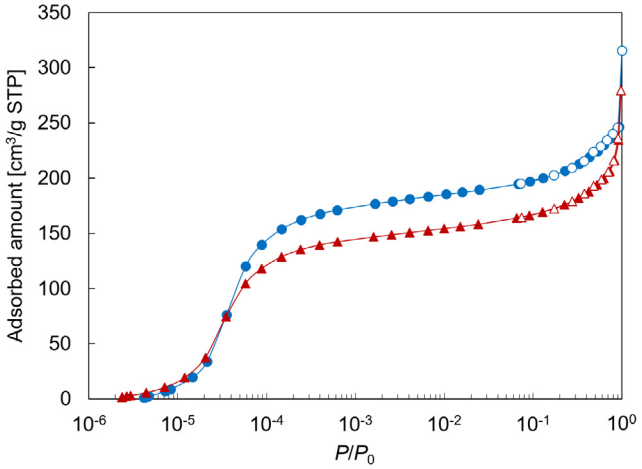

Fig. 3. Ar adsorption/desorption isotherms at 87 K of parent (triangle) and coated CHA (circle). Closed symbols: adsorption, open symbols: desorption.

3.4. Separation of ABE mixtures

Next, we evaluated the effect of competitive adsorption in the separation of ABE mixtures in humid conditions on both materials. Fig. 7 depicts the breakthrough profiles of the ABE mixture on the parent and coated CHA at 313 K. As observed in earlier work [21], acetone shows immediate breakthrough on both materials, indicating its molecular size is too large to allow entrance to the 8 membered ring pores of CHA. Subsequently, steep and almost immediate breakthrough of 1-butanol was observed, again showing that this compound is almost not adsorbed. Ethanol is adsorbed more strongly and breaks through much later, with a broader concentration profile.

Comparing with the profiles obtained with the binary mixture of ethanol and water vapor (open symbols in Fig. 7), the breakthrough profiles of ethanol were significantly broadened in presence of acetone and 1-butanol, although both last compounds are nearly not adsorbed. Such an effect was observed before on SAPO-34, a structural analogue of chabazite. Cousin Saint Remi et al. found that the time constant of ethanol was lowered by one order magnitude in presence of 1-propanol. In these narrow pore zeolites, counterdiffusion effects play an important role; the diffusion rate of the fast diffusing species decreases as the number of slow diffusing molecules increases [17,36]. Considering that acetone is too large to diffuse into the pores of CHA, competitively adsorbed 1-butanol, with extremely slow diffusivity (diffusion constant of butanol is 5 orders of magnitude smaller than that of ethanol [17], restricts the diffusion of ethanol, resulting in broadened breakthrough profiles of ethanol (see Fig. S1). This effect is more pronounced in the coated sample, again pointing at a slower diffusion mechanism on this material.

Additionally, the presence of 1-butanol or acetone shifts the ethanol breakthrough curves to the left, corresponding to a significant decrease in adsorbed amounts, by about 30%, as listed in Table 2. DFT calculations show that, energetically, the most stable state corresponds to two to three molecules of ethanol adsorbed per cage [21]. Also Krishna and van Baten reported that the ethanol loading is approximately two molecules per cage at low partial pressure (< 1000 Pa) and 300 K [16]. In the current experiments, the adsorbed amount of ethanol at 313 K in the binary mixture was 1.66 and 1.59 molecules per cage for the parent

Table 1
Physical properties of parent and coated CHA.

	Relative crystallinity[b]	Si/Al[a]	Si/Al of small crystals[a]	Average crystal sizes [μm]	Micropore volume [cm^3/g][c]
Parent CHA	100	39.3	–	3.87	0.22
Coated CHA	113	40.6	∞	4.06	0.26

[a] measured by EDX, [b]based on (1 0 0) [c]calculated by the Gurvich rule

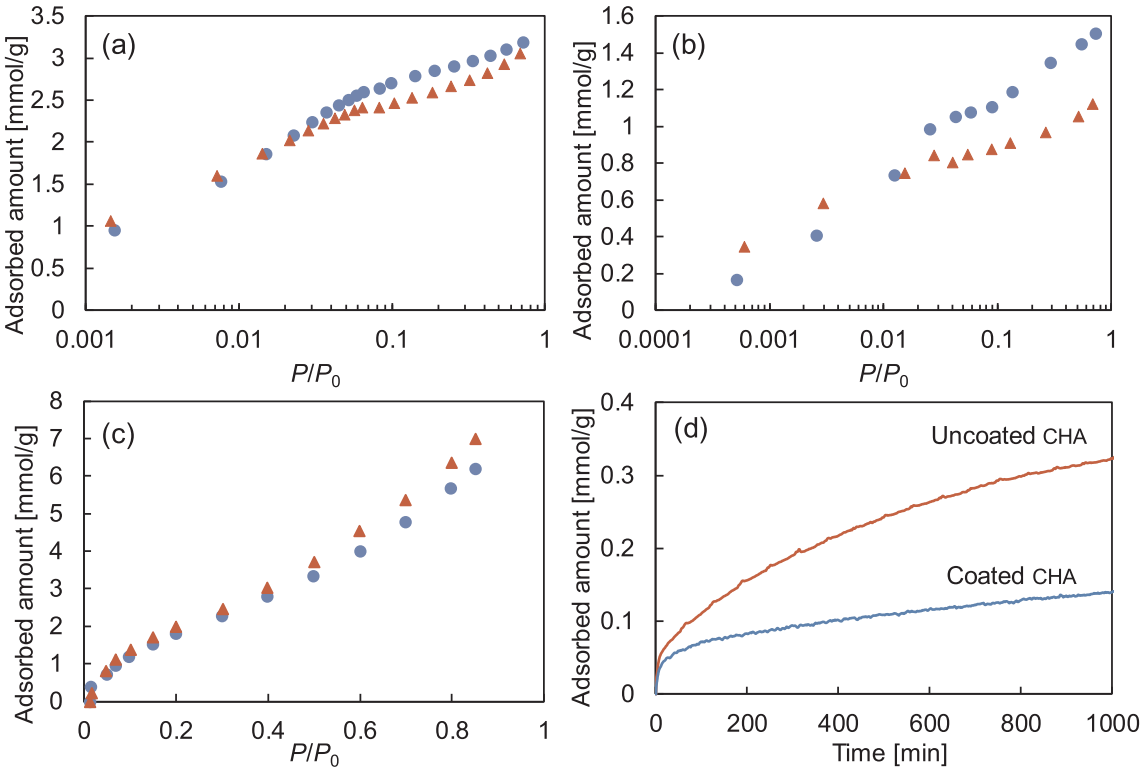

Fig. 4. Vapor phase adsorption isotherms of ethanol (a), 1-butanol (b), water (c) and uptake kinetics (d) at the first point in the 1-butanol isotherms on the parent (triangle) and coated CHA (circle) at 313 K.

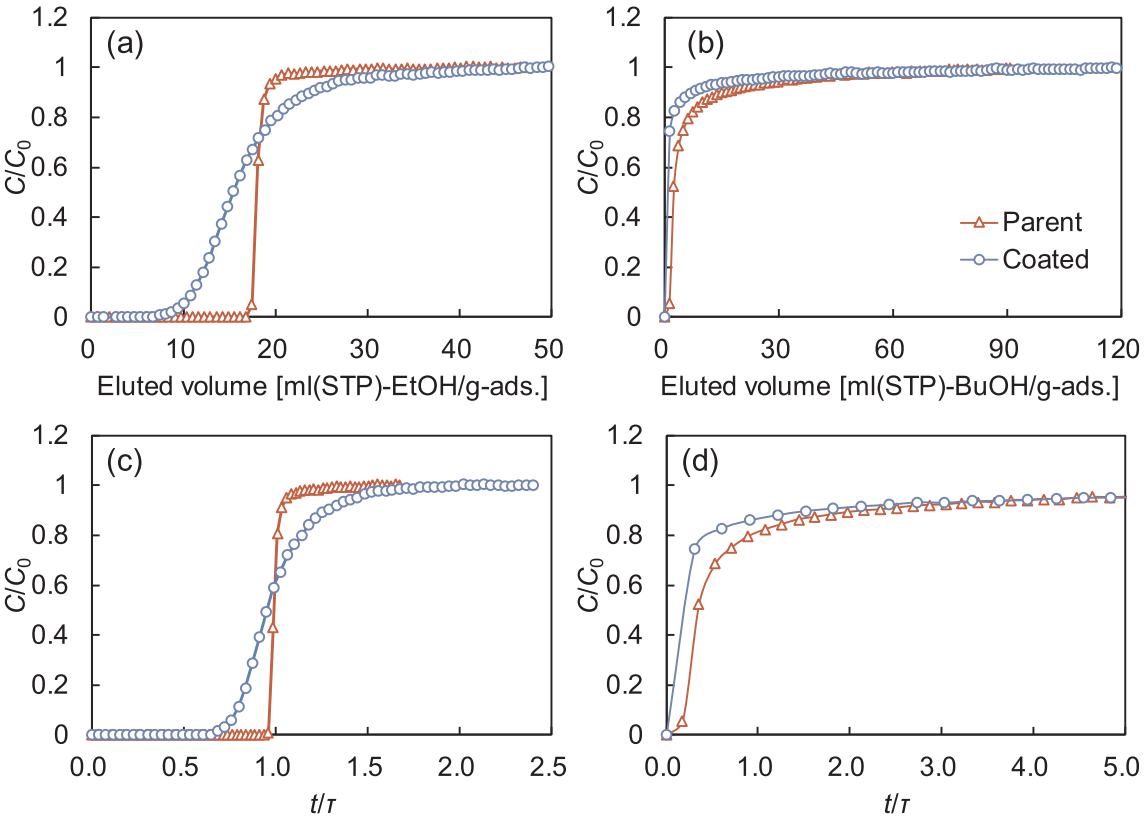

Fig. 5. Breakthrough profiles of ethanol (a and c) and 1-butanol (b and d) on parent (triangle) and coated CHA (circle) at 373 K in humid condition. P_{EtOH} = 190 Pa, P_{BuOH} = 310 Pa, P_{H2O} = 4.2 kPa. Figures (c) and (d) show normalized breakthrough curves, in which the breakthrough time was divided by the average breakthrough time as calculated by integration of the breakthrough curve.

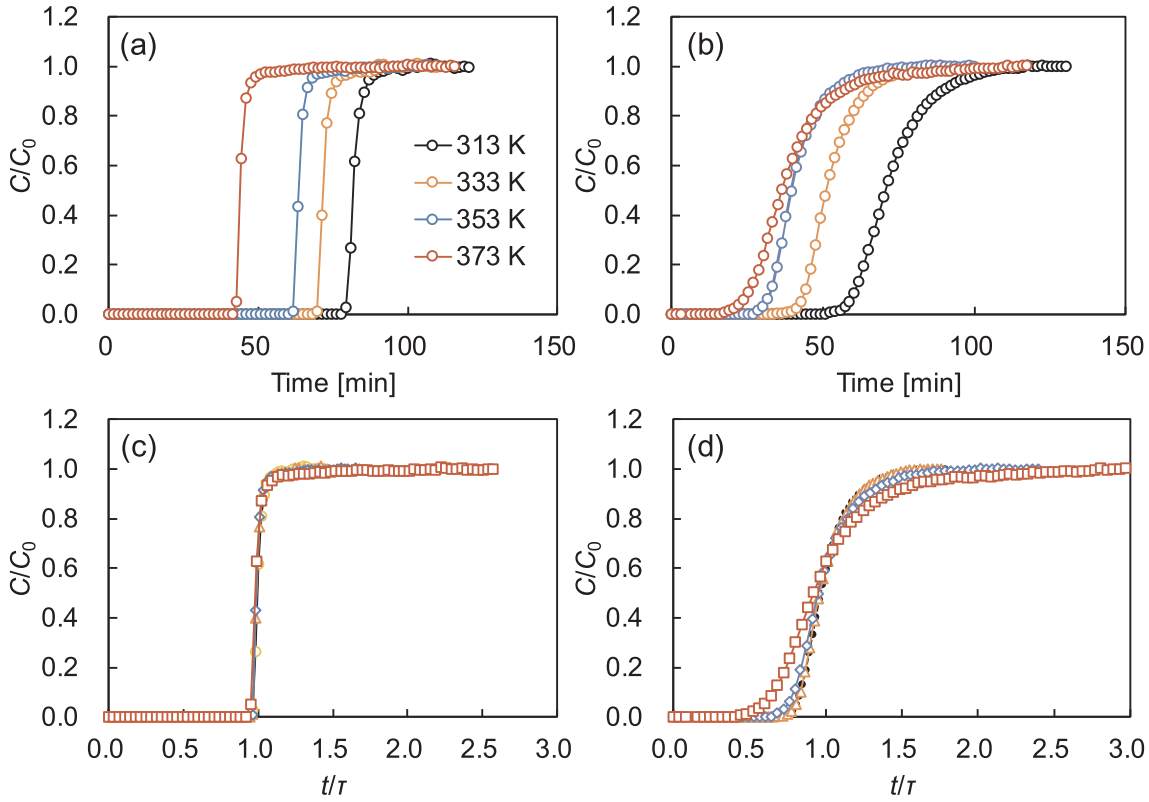

Fig. 6. Breakthrough profiles of ethanol on parent (a and c) and coated CHA (b and d) in different temperatures and humid condition. P_{EtOH} = 190 Pa, P_{H2O} = 4.2 kPa.

and coated CHA, which is in line with those calculations. Thus, the competitive adsorption and diffusion mechanism is hypothesized as follows. Initially, kinetically preferred ethanol molecules would first adsorb in the chabazite cages, with a loading of two molecules per cage. With increasing contact time, those ethanol molecules are gradually replaced by slowly adsorbing 1-butanol molecules. In fact, the breakthrough curve of butanol approaches the feed concentration very gradually after its steep rising and the decreased amount of adsorbed ethanol (when shifting from the binary to the quaternary mixture) corresponds to 2–3 times the number of adsorbed 1-butanol molecules in the quaternary mixture.

Another series of experiments was performed using a mixture composition corresponding to that of the vapor phase above a fermentation broth [21]. The experimental conditions were identical to those in the previous experiment except for the ethanol partial pressure (decreased to 50 Pa from 200 Pa). Fig. 8 shows the typical breakthrough profiles of ABE and water on the parent CHA and coated CHA, respectively. Almost immediate breakthrough of acetone is observed on both materials, but interestingly, a larger roll-up of the acetone concentration is observed on the parent CHA as compared to the coated CHA. On the coated CHA, both 1-butanol and acetone break through immediately, while a short delay between acetone and butanol is observed with the parent CHA. Thus, the coated CHA behaves even more selective and shows larger exclusion of acetone and 1-butanol. Possibly, the growth of the all-Si chabazite coating reduces surface adsorption of acetone, which is in line with the reduced surface activity of the coated CHA in xylene cracking (vide supra). Water retention is comparable on both zeolites.

Basically, the breakthrough profiles of acetone and 1-butanol using model ABE mixture were similar to those obtained at high ethanol partial pressure. However, the breakthrough profiles of ethanol became much broader with decreasing ethanol partial pressure. This can be

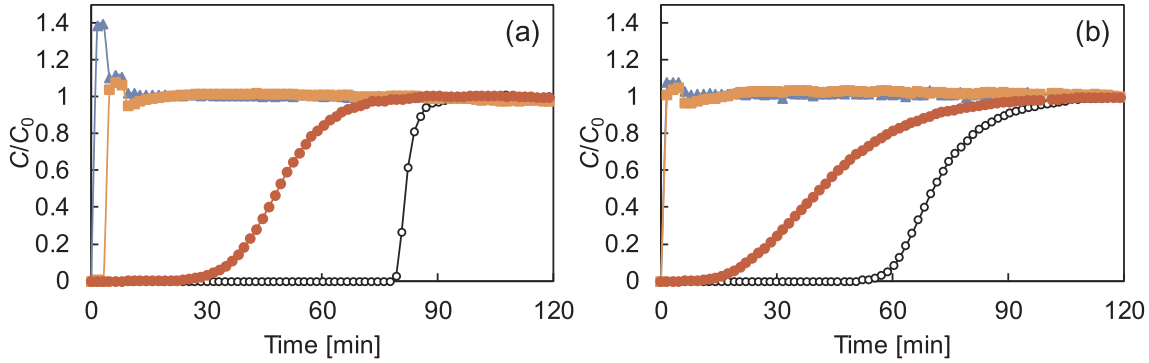

Fig. 7. Breakthrough profiles of acetone (triangle), 1-butanol (square) and ethanol (circle) on the parent (a) and coated CHA (b) using ABE mixture in humid conditions at 313 K. $P_{Acetone}$ = 200 Pa, P_{EtOH} = 200 Pa, P_{BuOH} = 300 Pa, P_{H2O} = 4.2 kPa. Filled symbols: quaternary mixture of ABE and water vapor, open symbols: ethanol (P_{EtOH} = 190 Pa) in a binary mixture of ethanol and water vapor (P_{H2O} = 4.2 kPa).

Table 2
Adsorbed amount of alcohols and separation factor in binary and quaternary mixtures.

	Temperature [K]	Parent CHA			Coated CHA		
		Adsorbed amount [mmol/g]		$\alpha_{EtOH/BuOH}$	Adsorbed amount [mmol/g]		$\alpha_{EtOH/BuOH}$
		EtOH	1-BuOH		EtOH	1-BuOH	
Binary	313	1.51	–		1.46	–	
Quaternary	313	1.09	0.19	8.8	1.12	0.12	14.1

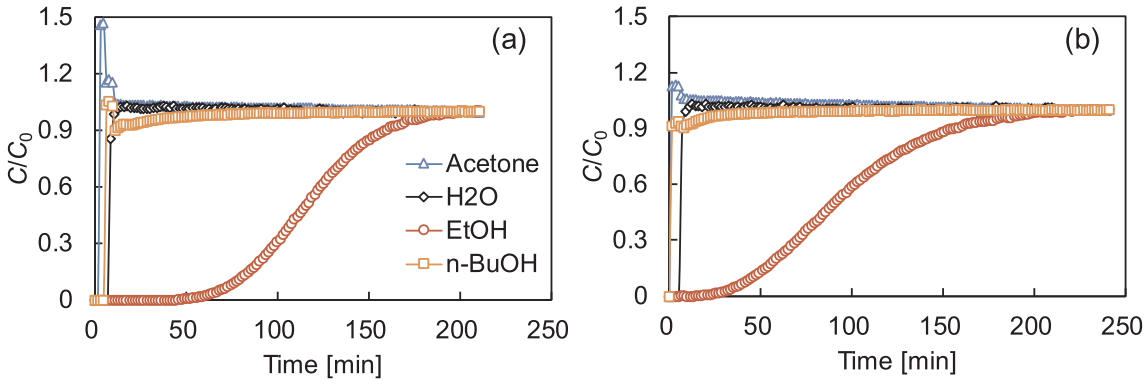

Fig. 8. Breakthrough profiles of ethanol (circle), 1-butanol (square), acetone (triangle) and water (rhombus) on the parent (a) and coated CHA (b) with a total flow rate of 40 cm^3-stp/min at 313 K. Mixture composition: P_{EtOH} = 50 Pa, P_{BuOH} = 300 Pa, $P_{Acetone}$ = 190 Pa and P_{H2O} = 4.2 kPa.

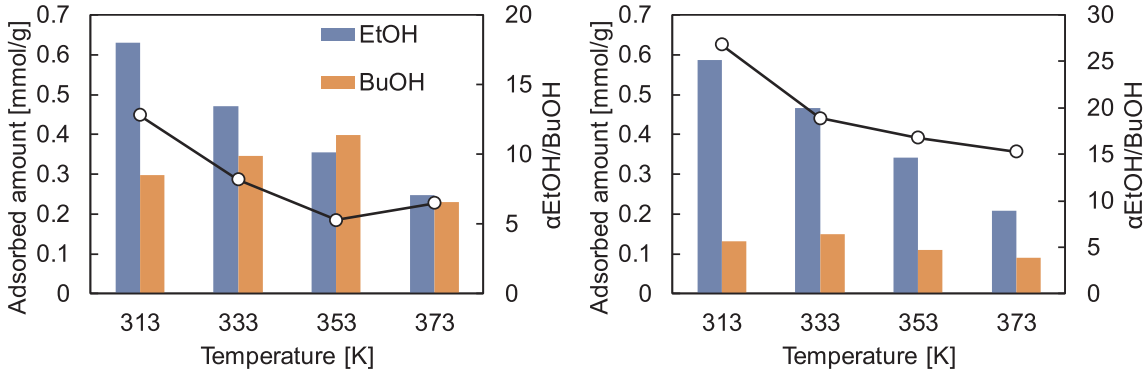

Fig. 9. Separation factor of ethanol over 1-butanol and their adsorbed amount on the parent (left) and coated CHA (right) in different temperatures. Mixture composition: P_{EtOH} = 50 Pa, P_{BuOH} = 300 Pa, $P_{Acetone}$ = 190 Pa and P_{H2O} = 4.2 kPa.

explained by the lower driving force of ethanol adsorption at lower pressure. Comparing the breakthrough profiles of the coated CHA to the parent material, the breakthrough profile of ethanol became broader, and that of 1-butanol became sharper with a significant decrease in the breakthrough time at C/C_0 = 0.05 from 4.9 min to 0.1 min. This trend is in line with the case of the binary mixture (Fig. 5). It should be noted that the broadened ethanol profile as a result of the Si-CHA coating negatively affects the material performance, for example in the two-step adsorptive separation of ABE mixtures reported in the literature [21].

Fig. 9 shows the separation factor and adsorbed amount of ethanol and 1-butanol at different adsorption temperatures. Like in the previous case, the adsorbed amounts of ethanol were comparable for the parent and coated material and decrease with temperature. In contrast, the adsorbed amount of 1-butanol differ significantly, from 0.28 mmol/g for the parent CHA to 0.12 mmol/g for the coated CHA at 313 K. As a result of that, the coated CHA exhibited a larger separation factor of ethanol over 1-butanol ($\alpha_{EtOH/BuOH}$ = 13.8 and 30.6 for the parent and coated CHA, respectively).

Moreover, in the case of the parent CHA, a pronounced effect of temperature on 1-butanol uptake is observed: the adsorbed amount of 1-butanol increased from 0.28 mmol/g to 0.40 mmol/g with an increase in temperature from 313 K to 353 K. This is explained by an improved 1-butanol diffusivity at higher temperature (kinetic effect) on the parent CHA, offsetting the negative thermodynamic effect on equilibrium capacity. The parent CHA thus becomes less selective when increasing temperature from 313 K to 353 K. At even higher temperature, the butanol capacity decreased again. On the other hand, no effect of temperature on the uptake of 1-butanol on the coated CHA could be detected and amount adsorbed remained low at all temperatures.

These results indicate that the growth of a pure silica CHA coating around the Al containing CHA core resulted in an inhibition of diffusion into the material. Although the parent CHA already shows very slow diffusion of 1-butanol, leading to the selective adsorption of ethanol over 1-butanol, this effect is magnified on the coated CHA. The slower diffusion of 1-butanol on the coated CHA also affects the diffusion and adsorption of ethanol, resulting in broader breakthrough curves for ethanol.

4. Conclusions

We synthesized a core-shell structured CHA type zeolite, consisting

of a CHA type aluminosilicate coated with a pure silica CHA thin layer. The effect of the pure silica CHA coating on the vapor phase ABE separation was evaluated. While the adsorption capacity of ethanol was similar for both materials, the pure silica CHA coating unexpectedly had a negative impact on the ethanol uptake rate; significant broadening of the breakthrough profile was observed. The coated CHA showed a more discriminative behavior with respect to acetone and 1-butanol. The pure silica CHA coating possibly reduced the number of surface adsorption sites and resulted in a slower diffusion of 1-butanol. The growth of a pure silica CHA coating around the Al containing CHA core thus resulted in an inhibition of diffusion into the material. Due to a change in the transport mechanism, the temperature dependency of the separation behavior was also strongly affected. The exact reasons for the additional diffusion barrier are not yet understood. Possibly, the presence or absence of Al or a different level of defects in the outer layer affects the initial affinity and entrance of the molecules. Also a mismatch between coating and core could cause a mass transfer resistance. However, no straightforward methods are available to analyze the properties of the pores of the outer layer. Still, the current results demonstrate that the separation properties of a zeolite can be modified by adding a secondary zeolite layer.

Acknowledgement

This work was supported by JSPS KAKENHI Grant Number 15KK0234.

Appendix A. Supplementary data

Supplementary data to this article can be found online at https://doi.org/10.1016/j.cej.2019.01.106.

References

[1] Z. Liu, Y. Ying, F. Li, C. Ma, P. Xu, Butanol production by clostridium Beijerinckii ATCC 55025 from wheat bran, J. Ind. Microbiol. Biotech. 37 (2010) 495–501, https://doi.org/10.1007/s10295-010-0695-8.
[2] N. Abdehagh, F.H. Tezel, J. Thibault, Separation techniques in butanol production: challenges and developments, Biomass Bioenergy 60 (2014) 222–246, https://doi.org/10.1016/j.biombioe.2013.10.003.
[3] H.-J. Huang, S. Ramaswamy, Y. Liu, Separation and purification of biobutanol during bioconversion of biomass, Sep. Purif. Technol. 132 (2014) 513–540, https://doi.org/10.1016/j.seppur.2014.06.013.
[4] C. Xue, J. Zhao, C. Lu, S.-T. Yang, F. Bai, I.C. Tang, High-titer n-butanol production by clostridium acetobutylicum JB200 in fed-batch fermentation with intermittent gas stripping, Biotechnol. Bioeng. 109 (2012) 2746–2756, https://doi.org/10.1002/bit.24563.
[5] F. Raganati, A. Procentese, G. Olivieri, M. Elena Russo, P. Salatino, A. Marzocchella, Bio-butanol separation by adsorption on various materials: Assessment of isotherms and effects of other ABE-fermentation compounds, Sep. Purif. Technol. 191 (2018) 328–339, https://doi.org/10.1016/j.seppur.2017.09.059.
[6] R. Goerlitz, L. Weisleder, S. Wuttig, S. Trippel, K. Karstens, P. Goetz, H. Niebelschuetz, Bio-butanol downstream processing: regeneration of adsorbents and selective exclusion of fermentation by-products, Adsorption 24 (2018) 95–104, https://doi.org/10.1007/s10450-017-9918-x.
[7] C. Xue, F. Liu, M. Xu, I.-C. Tang, J. Zhao, F. Bai, S.-T. Yang, Butanol production in acetone-butanol-ethanol fermentation with in situ product recovery by adsorption, Bioresour. Technol. 219 (2016) 158–168, https://doi.org/10.1016/j.biortech.2016.07.111.
[8] N. Abdehagh, F.H. Tezel, J. Thibault, Adsorbent screening for biobutanol separation by adsorption: kinetics, isotherms and competitive effect of other compounds, Adsorption 19 (2013) 1263–1272, https://doi.org/10.1007/s10450-013-9566-8.
[9] A. Oudshoorn, L.A.M. van der Wielen, A.J.J. Straathof, Adsorption equilibria of bio-based butanol solutions using zeolite, Biochem. Eng. J. 48 (2009) 99–103, https://doi.org/10.1016/j.bej.2009.08.014.
[10] J. Cousin Saint Remi, G. Baron, J. Denayer, Adsorptive separations for the recovery and purification of biobutanol, Adsorption 18 (2012) 367-373. https://doi.org/10.1007/s10450-012-9415-1.
[11] C. Gao, J. Wu, Q. Shi, H. Ying, J. Dong, Adsorption breakthrough behavior of 1-butanol from an ABE model solution with high-silica zeolite: Comparison with zeolitic imidazolate frameworks (ZIF-8), Microporous Mesoporous Mater. 243 (2017) 119–129, https://doi.org/10.1016/j.micromeso.2017.02.009.
[12] C. Gao, Q. Shi, J. Dong, Adsorptive separation performance of 1-butanol onto typical hydrophobic zeolitic imidazolate frameworks (ZIFs), CrystEngComm 18 (2016) 3842–3849, https://doi.org/10.1039/C6CE00249H.
[13] J. Cousin Saint Remi, T. Rmy, V. Van Hunskerken, S. Van de Perre, T. Duerinck, M. Maes, D. De Vos, E. Gobechiya, C.E.A. Kirschhock, G.V. Baron, J.F.M. Denayer, Biobutanol separation with the metal–organic framework ZIF-8, Chemsuschem 4 (2011) 1074–1077, https://doi.org/10.1002/cssc.201100261.
[14] I. Daems, R. Singh, G. Barona, J. Denayer, Length exclusion in the adsorption of chain molecules on chabazite type zeolites, Chem. Commun. (2007) 1316–1318, https://doi.org/10.1039/b615661d.
[15] T. Remy, J. Cousin Saint Remi, R. Singh, P.A. Webley, G.V. Baron, J.F.M. Denayer, Adsorption and separation of C1–C8 alcohols on SAPO-34, J. Physc. Chem. C 115 (2011) 8117–8125, https://doi.org/10.1021/jp111615e.
[16] R. Krishnaa, J.M. van Baten, Entropy-based separation of linear chain molecules by exploiting differences in the saturation capacities in cage-type zeolites, Sep. Purif. Technol. 76 (2011) 325–330, https://doi.org/10.1016/j.seppur.2010.10.023.
[17] J. Cousin Saint Remi, G.V. Baron, J.F.M. Denayer, Nonuniform chain-length-dependent diffusion of short 1-alcohols in SAPO-34 in liquid phase, J. Phys. Chem. C 117 (2013) 9758–9765, https://doi.org/10.1021/jp312287k.
[18] N. Abdehagh, B. Dai, J. Thibault, F.H. Tezel, Biobutanol separation from ABE model solutions and fermentation broths using a combined adsorption–gas stripping process, J. Chem. Technol. Biotechnol. 92 (2017) 245–251, https://doi.org/10.1002/jctb.4977.
[19] Y. Cao, K. Wang, X. Wang, Z. Gu, W. Gibbons, H. Vu, Adsorption of butanol vapor on active carbons with nitric acid hydrothermal modification, Bioresour. Technol. 196 (2015) 525–532, https://doi.org/10.1016/j.biortech.2015.08.027.
[20] Y. Cao, K. Wang, X. Wang, Z. Gu, W. Gibbons, H. Vu, Butanol vapor adsorption behavior on active carbons and zeolite crystal, Appl. Surface Sci. 349 (2015) 1–7, https://doi.org/10.1016/j.apsusc.2015.05.005.
[21] S. Van der Perre, P. Gelin, B. Claessens, A. Martin-Calvo, J. Cousin Saint Remi, T. Duerinck, G.V. Baron, M. Palomino, L.Y. Sánchez, S. Valencia, J. Shang, R. Singh, P.A. Webley, F. Rey, J.F.M. Denayer, Intensified biobutanol recovery by using zeolites with complementary selectivity, Chemsuschem 10 (2017) 2968–2977, https://doi.org/10.1002/cssc.201700667.
[22] M. Miyamoto, T. Kamei, N. Nishiyama, Y. Egashira, K. Ueyama, Single crystals of ZSM-5/silicalite composites, Adv. Mater. 17 (2005) 1985–1988, https://doi.org/10.1002/adma.200500522.
[23] D.V. Vu, M. Miyamoto, N. Nishiyama, Y. Egashira, K. Ueyama, Selective formation of *para*-xylene over H-ZSM-5 coated with polycrystalline silicalite crystals, J. Catal. 243 (2006) 389–394, https://doi.org/10.1016/j.jcat.2006.07.028.
[24] M. Miyamoto, K. Mabuchi, J. Kamada, Y. Hirota, Y. Oumi, N. Nishiyama, S. Uemiya, *para*-Selectivity of silicalite-1 coated MFI type galloaluminosilicate in aromatization of light alkanes, J. Porous Mater. 22 (2015) 769–778, https://doi.org/10.1007/s10934-015-9950-8.
[25] M. Miyamoto, S. Ono, K. Kusukami, Y. Oumi, S. Uemiya, High water tolerance of a core–shell-structured zeolite for CO_2 adsorptive separation under wet conditions, Chemsuschem 11 (2018) 1756–1760, https://doi.org/10.1002/cssc.201800063.
[26] Y. Bouizi, I. Diaz, L. Rouleau, V.P. Valtchev, Core-shell zeolite microcomposite, Adv. Funct. Mater. 15 (2005) 1955–1960, https://doi.org/10.1021/cm0611744.
[27] Y. Bouizi, L. Rouleau, V.P. Valtchev, Factors controlling the formation of core−-shell zeolite−zeolite composites, Chem. Mater. 18 (2006) 4959–4966, https://doi.org/10.1021/cm0611744.
[28] G.D. Pirngruber, C. Laroche, M. Maricar-Pichon, L. Rouleau, Y. Bouizi, V. Valtchev, Microporous Mesoporous Mater. 169 (2013) 212–217, https://doi.org/10.1016/j.micromeso.2012.11.016.
[29] T. Du, H. Qu, Q. Liu, Q. Zhong, W. Ma, Synthesis, activity and hydrophobicity of Fe-ZSM-5@silicalite-1 for NH_3-SCR, Chem. Eng. J. 262 (2015) 1199–1207, https://doi.org/10.1016/j.cej.2014.09.119.
[30] J. Huang, J. Hu, W. Du, H. Liu, F. Qian, M. Wang, Ultrafast synthesis of 13X@NaA composites through plasma treatment for highly selective carbon capture, J. Mater. Chem. A 5 (2017) 18801–18807, https://doi.org/10.1039/c7ta05649d.
[31] C. Yang, X. Meng, D. Yi, Z. Ma, N. Liu, L. Shi, Cu^{2+} modified silicalite-1/NaY structure for the adsorption desulfurization of dimethyl disulfide from methyl tert-butyl ether, Ind. Eng. Chem. Res. 57 (2018) 9162–9170, https://doi.org/10.1021/acs.iecr.8b01211.
[32] M. Miyamoto, T. Nakatani, Y. Fujioka, K. Yogo, Verified synthesis of pure silica CHA-type zeolite in fluoride media, Microporous Mesoporous Mater. 206 (2015) 67–75, https://doi.org/10.1016/j.micromeso.2014.12.012.
[33] S. Tanaka, K. Fujita, Y. Miyake, M. Miyamoto, Y. Hasegawa, T. Makino, S. Van der Perre, J. Cousin Saint Remi, T. Van Assche, G.V. Baron, J.F.M. Denayer, Adsorption and diffusion phenomena in crystal size engineered ZIF-8 MOF, J. Phys. Chem. C 119 (2015) 28430–28439, https://doi.org/10.1021/acs.jpcc.5b09520.
[34] V. Finsy, H. Verelst, L. Alaerts, D. De Vos, P.A. Jacobs, G.V. Baron, J.F.M. Denayer, Pore-filling-dependent selectivity effects in the vapor-phase separation of xylene isomers on the metal-organic rramework MIL-47, J. Am. Chem. Soc. 130 (2008) 7110–7118, https://doi.org/10.1021/ja800686c.
[35] J.H. Kim, T. Kunieda, M. Niwa, Generation of shape-selectivity of p-xylene formation in the synthesized ZSM-5 zeolites, J. Catal. 173 (1998) 433–439, https://doi.org/10.1006/jcat.1997.1950.
[36] T. Masuda, Y. Fujikata, H. Ikeda, K. Hashimoto, Diffusivities in the binary components system within MFI-type zeolite crystals, Microporous Mesoporous Mater. 38 (2000) 323–332, https://doi.org/10.1016/S1387-1811(00)00151-7.